



ISSN: 0975-833X

RESEARCH ARTICLE

SURFACE AREA ANALYSIS AND GAS TRANSPORT PROPERTIES WITH INORGANIC CERAMIC MEMBRANES

Edidiong Okon, Mohammed Nasir Kajama, Habiba Shehu, Ngozi Nwogu and *Edward Gobina

Center for Process Integration and Membrane Technology (CPIMT), School of Engineering,
The Robert Gordon University Aberdeen, AB10 7GJ, United Kingdom

ARTICLE INFO

Article History:

Received 22nd August, 2014
Received in revised form
19th September, 2014
Accepted 24th October, 2014
Published online 18th November, 2014

Key words:

Gas transport,
Nitrogen adsorption/desorption,
Ceramic membrane,
Permeance,
BET isotherm.

ABSTRACT

This work presents gas transport properties through inorganic ceramic membrane. The characterization of the pore size distribution and the specific surface area of the porous ceramic membrane were carried out using Liquid Nitrogen adsorption at the temperature of 77K. Both modified and unmodified inorganic porous ceramic membranes were used for the analysis for the purpose of comparison. The surface area of the unmodified and modified membrane was determined using Brunauer-Emmett-Teller (BET) isotherm, whereas the pore diameter of both membranes was determined using Barrette-Joyner-Halenda (BJH) curve. The adsorption/desorption curve for the modified membrane showed a type IV/V isotherm, characteristic of a mesoporous structure whereas the specific area of the unmodified ceramic membrane represents a type III isotherm indicating a microporous structure. The examination of the surface morphology of the silica membrane was also analysed using scanning electron microscopy (SEM). Single gases used for the analysis include: Argon (Ar), helium (He), nitrogen (N₂) and carbon dioxide (CO₂). The gas permeance decreases with respect to gauge pressure (bar) at 393 K in the order of the gas molecular weight i.e CO₂>Ar>N₂>He indicating Knudsen mechanism.

Copyright © 2014 Edidiong Okon et al. This is an open access article distributed under the Creative Commons Attribution License, which permits unrestricted use, distribution, and reproduction in any medium, provided the original work is properly cited.

INTRODUCTION

In recent decades, the application of membrane in the chemical industry has received a lot of attention (Peter *et al.*, 2004). Membrane-based separations are cost effective and energy efficient (Tsai *et al.*, 2000). The use of porous silica membrane has grown continuously because of their excellent properties including large mechanical and thermal stability, high surface area, precisely specific size of pores and particles, easy surface modification and also large pore volume (Choma *et al.*, 2003). Based on the IUPAC (International Union of Pure and Applied Chemistry) approvals, membrane pores are classified into three types: macropores (pore diameter >50nm), micropore (pore diameter < 2nm) and mesopores (pore diameter between 2-50 nm). Membranes may be classified by different ways. However, depending on the material that the membrane is made of, the most popular division is between organic and inorganic membranes. Ceramic membrane is categorised under inorganic membranes, as they are usually composed of oxides such as alumina (Al₂O₃) (Coronas and Santamaria 1999) (Dafinov *et al.*, 2002). Inorganic ceramic membrane provides advantages including thermal stability, mechanical resistance, non-swelling easy cleaning and chemical inactivity (Dafinov *et al.*, 2002). Different methods have been introduced for the

preparation of silica porous membrane including: chemical vapour decomposition, sol-gel and leaching methods. However, sol-gel technique have attracted a lot of attention due to its potential to precisely control the pore size and pore structure and also its excellent processibility (Tsai *et al.*, 2000). According to Smart *et al.* (2013), the most accurate and common technique for analysing the structure and pore size of a porous membrane is by using probe molecules to adsorb on the pore walls and/or condense within the pores themselves. Nitrogen adsorption at 77 K is a standard and widely used technique for the determination of pore size distribution, specific surface area and pore volume for meso and microporous membranes (Choma *et al.*, 2003). Figure 1 shows the schematic diagram describing the types of physisorption isotherms that are used to describe the pore size distribution, total surface area and the average pore size of porous membrane. Where B represents the monolayer adsorption capacity from which the surface area of the porous membrane sample can be determined (Smart *et al.*, 2013).

During the gas transport across the membrane, when the gas pressure is higher on one side of the membrane than the other, the transport of gas through the membrane can be described using five mechanisms including: surface diffusion, Knudsen diffusion, capillary condensation, viscous or poiseuille flow and molecular sieving mechanism (Sidhu and Cussler 2001).

*Corresponding author: Edward Gobina,

Center for Process Integration and Membrane Technology (CPIMT), School of Engineering, The Robert Gordon University Aberdeen, AB10 7GJ, United Kingdom.

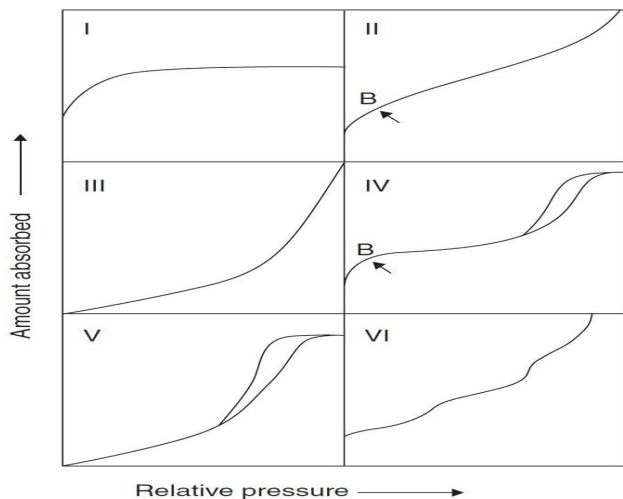


Fig. 1. Schematic representation of the types of physisorption isotherms for porous membrane (Smart *et al.*, 2013)

Knudsen diffusion mechanism takes place when the gas molecule diffuses into the pores and then moves around by colliding with the pore wall. However, this mechanism means that the mean free path (λ) of the permeating gas molecule is greater than the pore diameter (d) indicating that the Knudsen number is greater than 1. Viscous or poiseuille mechanism occurs when the mean free path of the gas molecule is smaller than the pore diameter. This means that the collision occurs only between the permeating gas molecules and in this case, Knudsen number is less than 1. However, viscous flow occurs in a larger pore and at higher pressure (Phattaranawik *et al.*, 2003). Capillary condensation occurs in a small pore. This mechanism of transport occur when a porous medium interact with a vapour, the saturation vapour pressure in the bulk (P_0) differs from the saturation vapour pressure in the pore (Sidhu and Cussler 2001). In surface diffusion, the adsorption of gas molecules are considered to be on the surface and move on the surface by jumping between the minimum potential energy generated on the membrane pore surface. Moreover, the diffusing gas molecules that bound on the surface may withdraw from their state of adsorption to the gaseous state if their kinetic energy is greater than their sorption energy (Lee and Oyama 2002). Hence, surface diffusion can only be useful at the relatively low temperature region that relies upon the sorption energy of the gas molecules. For molecular sieving to occur, the membrane must have pore diameters which are roughly the same as those of the gas molecules to be separated (Li 2007).

Experimental

The experimental analysis of the surface area and the pore diameter of the samples were determined based on a similar method as that of Smart *et al.* (2013) and Markovic *et al.* (2009) with some alteration in temperature and silica sol preparation process. The liquid nitrogen adsorption temperature was programmed at 77 K. The fragment of the silica α -Al₂O₃ ceramic membranes were crushed and used for the nitrogen adsorption analysis before and after dip-coating. Prior to the sample analysis, the degassing of the sample was carried out at 65 °C for 3h to clean the adsorbed contaminant from the system by introducing a vacuum or flow of inert gas

and preferably some heat. The weight of the sample cell before the degassing process was 27.7 g while the weight of the cell + unmodified membrane was 34.4g. The actual weight of the unmodified ceramic membrane was 6.30 g. However, for the modified ceramic membrane, the sample weight was 27.5 g, membrane + cell sample was 31.5 g, while the actual weight of the modified membrane was 3.50 g. Figure 2 shows a pictorial diagram of the nitrogen adsorption instrumentation that was used for the adsorption/desorption analysis and consists of the sample stations (1 and 2), dewar, sample cell, thermometer, and sample cell holder.

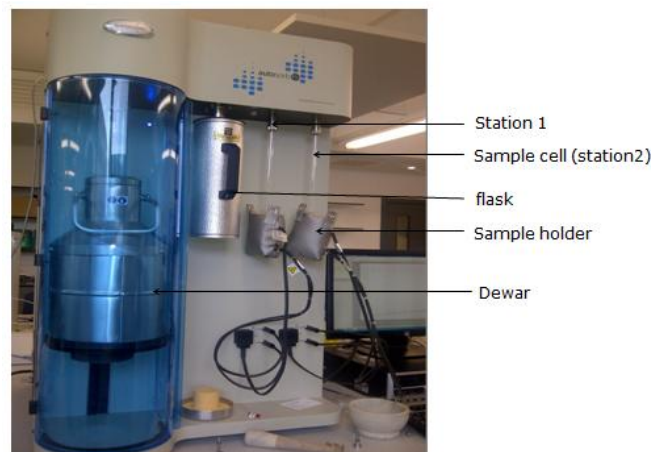


Fig. 2. Pictorial diagram of the Liquid Nitrogen adsorption at the Centre for Process Integration and Membrane Technology (CPIMT), RGU

The four gases that were used for the permeation tests were: argon (Ar), nitrogen (N₂), helium (He), and carbon dioxide (CO₂). The inner and the outer diameter of the ceramic membranes were 7mm and 10mm respectively while the total length was 36.6cm. The gas flow through the membrane was measured using a flow meter (Cole Parmer model) at the gauge pressure range of 0.10 – 1.00 bar and 393 K. The gases were supplied by BOC, UK. Figure 3 shows a schematic diagram of the gas permeation setup.

RESULTS AND DISCUSSION

The surface area of both the unmodified and modified silica ceramic membrane was analysed using nitrogen adsorption method to determine the surface area of the support and that of the silica modified sample. From the results obtained, it was observed that the surface area of the support was low as shown in Table 1 in contrast, the modified support indicated a 200% increase in the specific surface area. It was assumed that there could have been weak interaction between the adsorbing gas molecule and the support there by resulting in a low surface area. The results obtained for the BET isotherm for the support in Figure 4 showed a flat curve without hysteresis for both adsorption and desorption lines, indicating a type III isotherm. This suggests that the support was characteristic of a micropores structure (< 2nm pore size) which was in a good agreement with the type III isotherm. The plot of the amount of gas adsorbed (volume at STP (cc/g)) against the relative pressure (P/P_0) is shown in Figure 4 where the blue line represent desorption and the red line represent the adsorption line.

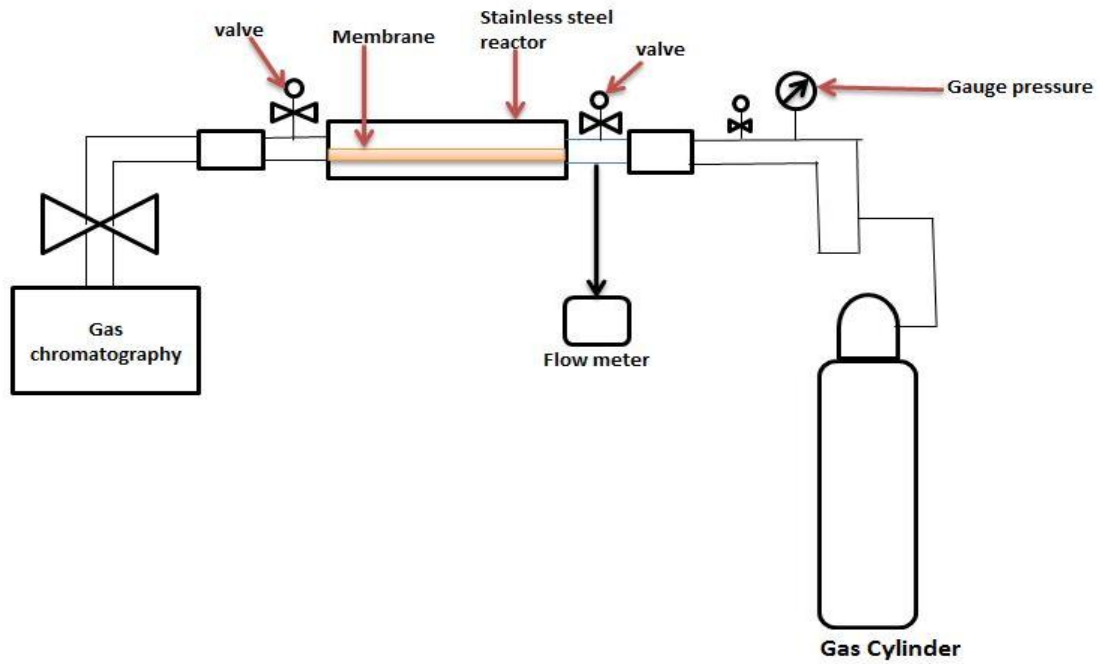


Fig. 3. Shows a schematic diagram of the gas permeation setup

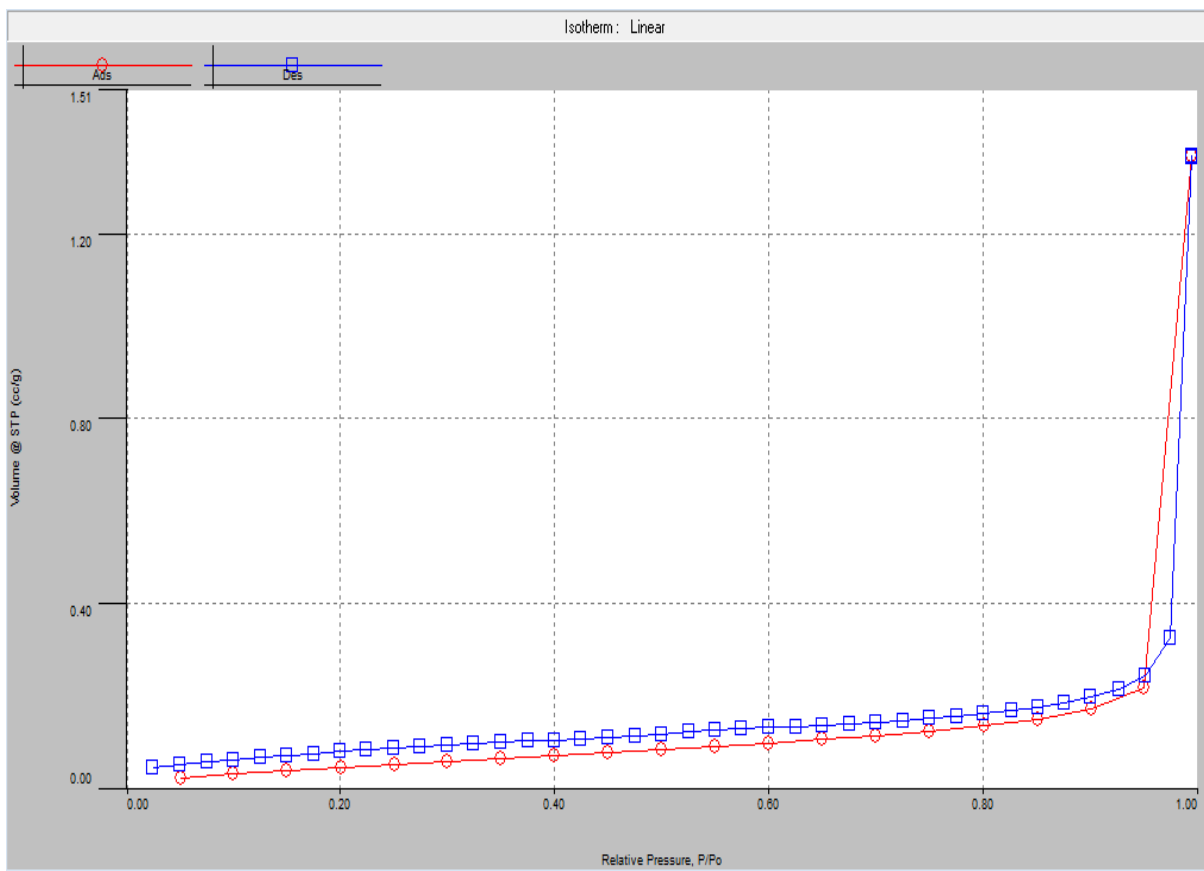


Fig. 4. Adsorption (blue)/desorption (red) isotherm of the surface support at 77K

In contrast to the support as shown in Table 1, the surface area of the modified membrane was found to be higher ($0.439\text{m}^2/\text{g}$) compared to the support ($0.206\text{m}^2/\text{g}$). According to Smart *et al.* (2013), the most significant isotherms used to explain porous ceramic membrane materials include type III isotherm which relates to the microporous solids and also type IV and V which corresponds to mesoporous solids usually ceramics undergoing hysteresis and capillary condensation during desorption. However, the results obtained in Figure 5 showed that the adsorption/desorption curves was in a good agreement with the type IV and Visotherm which was characteristic of mesopores structure with hysteresis. A similar result was obtained by Kuroaka *et al.* (2001) in their work using modified silica membrane used for the analysis exhibited a type IV isotherm based on the BET classification, indicating that the isotherm is a typical of adsorption on mesoporous solid which is characterised by hysteresis.

Figure 5 shows the adsorption/desorption isotherm for silica membrane. After the dip-coating process, the membrane pore size was expected to reduce in order to allow the penetration of the gas molecule across the membrane. However, from the results obtained for the pore diameter analysis, it was observed that the pore diameter of the modified ceramic membrane was found to be higher than the support as shown in Table 1. This could indicate the effect of the silica solution that was used in modifying the ceramic membrane. The BET and BJH values for the silica membrane and the support sample are shown in Table 1.

Table 1. BET and BJH values for modified and unmodified silica membrane

Sample	BET	BJH	
	Surface area (m^2/g)	Pore diameter (nm)	Pore Volume (cc/g)
unmodified	0.206	4.175	0.002
modified	0.439	4.179	0.008

The plot of the amount of gas adsorbed (volume at STP (cc/g)) against the relative pressure (P/P_0) is shown in Figure 5 below.

Figure 6 shows the BJH graph the support. Comparing the BJH curve for both the support and the silica membrane in Figure 6 and 7, it was found that the adsorption and desorption decreases with the change in volume for the support in Figure 6. This could have been as the result of the small pores ($< 2\text{nm}$) of the membrane which correspond to the BET isotherm with the result that the membrane was a microporous structure.

However, the reverse was the case for the BJH curve for the silica membrane in Figure 7. This also confirms that the silica membrane was a mesoporous structure ($2\text{-}50\text{nm}$). Figure 6 and 7 shows the BJH curves for the support and silica membrane at 77K .

The relationship between the gas permeance and the gauge pressure was also determined as shown in Figure 8.

From the graph of flux ($\text{molm}^{-2}\text{s}^{-1}$) against the gauge pressure (bar) in Figure 8, it was found that the gas flux increases with increase in gauge pressure at 393K indicating that viscous flow was the dominant transport mechanism. The R^2 value for the four gases was up to 0.99 indicating good correlation values for the gases. The graph of permeance against gauge pressure was also plotted to determine the flow mechanism of the different gases. From figure 9 it was found that the gas permeance initially decreases with gauge pressure at 393K . CO_2 gas showed the highest permeance at 0.10 bar in contrast to all the gases. It was observed that the gas permeance with respect to gauge pressure follow the trend of the gas molecular weight. The order of the gas permeance from the highest to the lowest was CO_2 ($44\text{g}/\text{mol}$) $>$ Ar ($40\text{g}/\text{mol}$) $>$ N_2 ($28\text{g}/\text{mol}$) $>$ He ($4\text{g}/\text{mol}$) as shown in Figure 9. This suggests that Knudsen mechanism of transport which relates to the gas molecular weight was the dominant flow mechanism of transport.

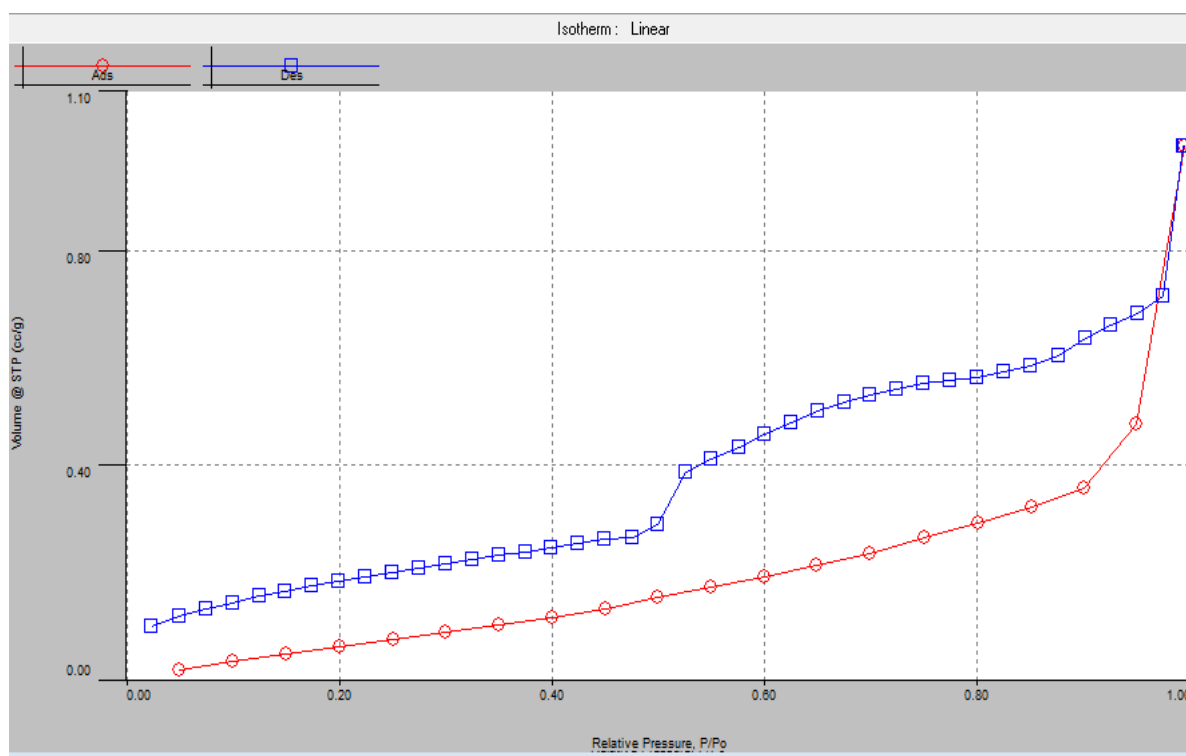


Fig. 5. Gas adsorption/desorption graph for an unmodified membrane at 77K

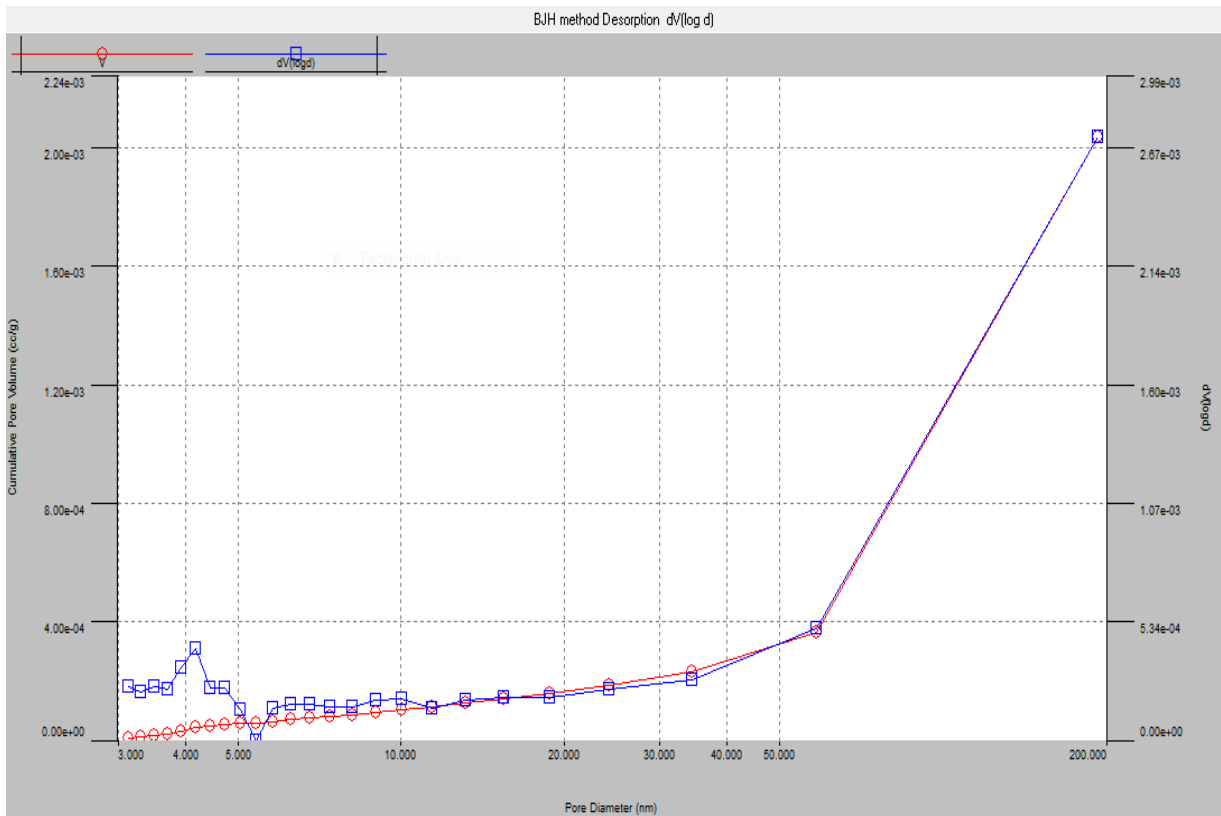


Fig. 6. BJH curve for the unmodified ceramic membrane at 77 K

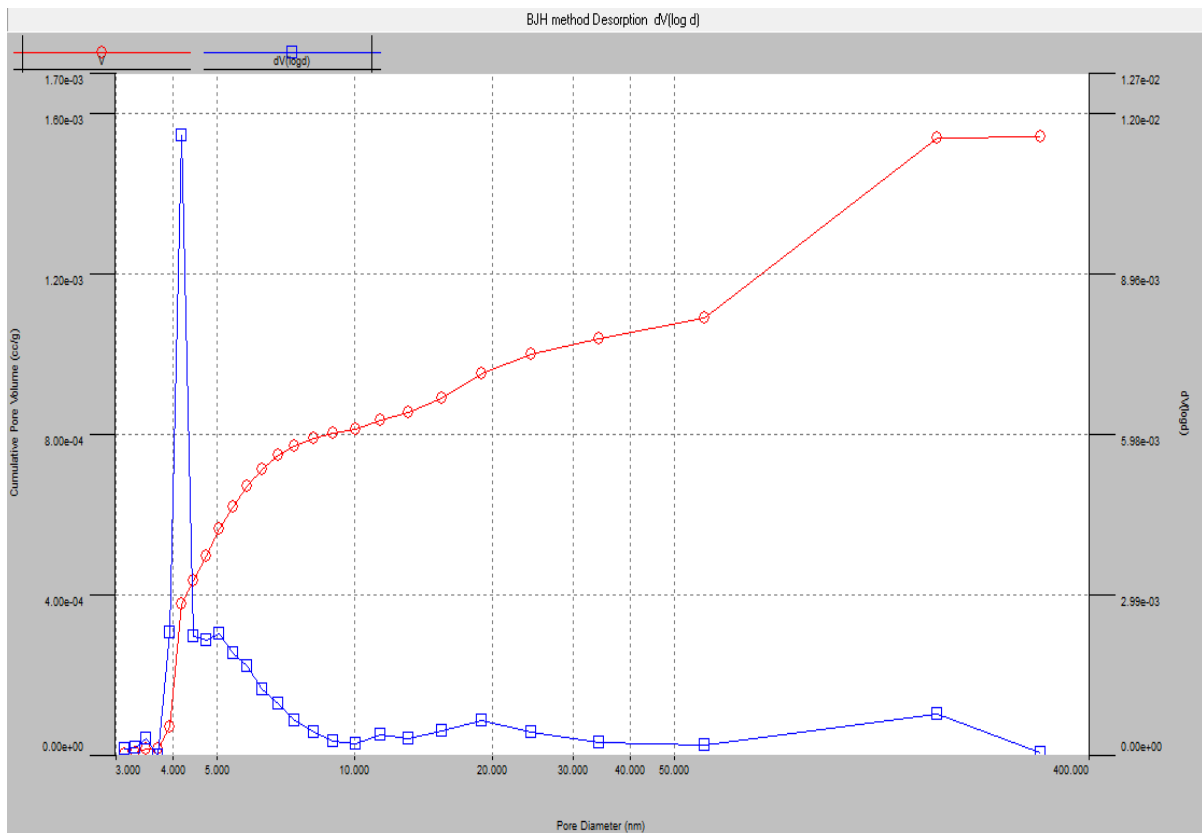


Fig. 7. BJH curve for the modified membrane at 77K

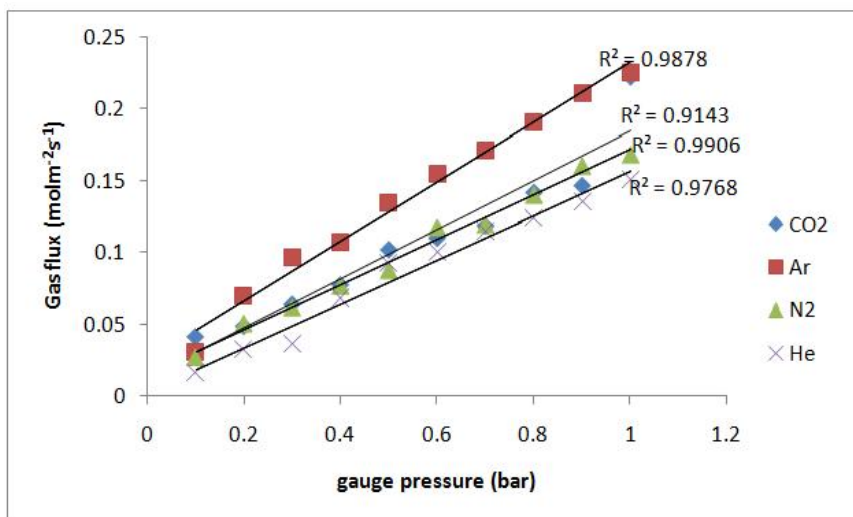


Fig. 8. Gas flux ($\text{molm}^{-2}\text{s}^{-1}$) against gauge pressure (bar) at 393 K

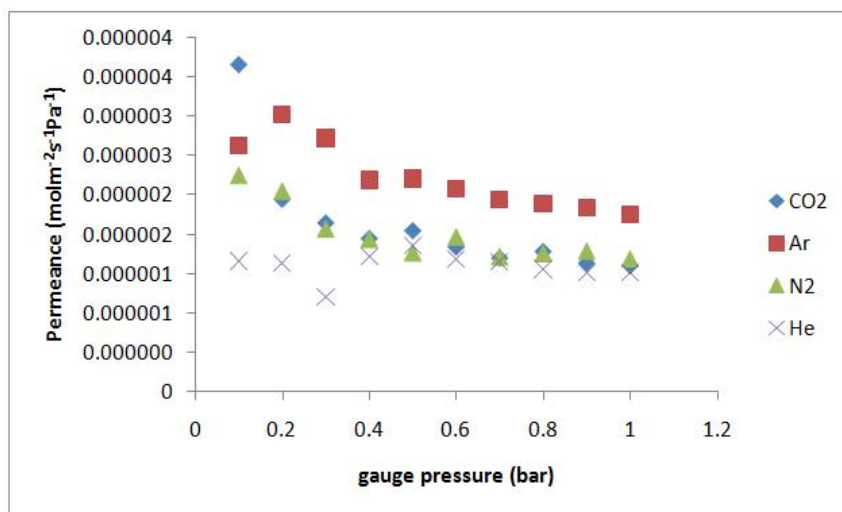


Fig. 9. Gas permeance ($\text{molm}^{-2}\text{s}^{-1}\text{Pa}^{-1}$) with gauge pressure (bar) at 393 K

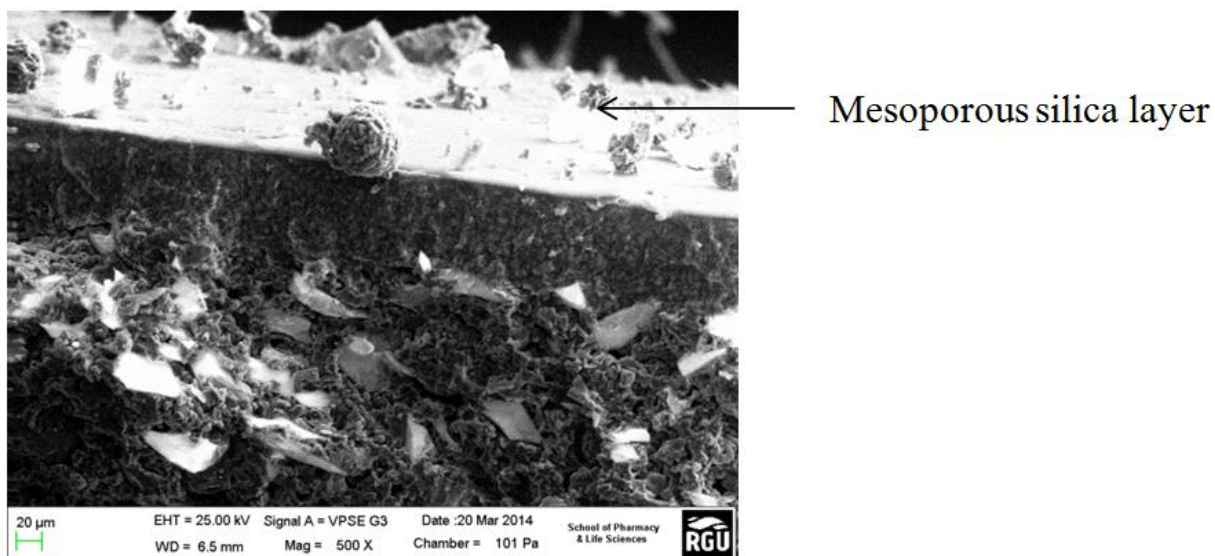


Fig. 10. SEM interior surface image of modified ceramic membrane

However, this result further confirms that the membrane was a defect-free membrane with the formation of mesopores layer.

The silica membrane was further analysed using scanning electron microscopy (SEM) to examine the surface morphology. From the result obtained in figure 10 it was found that the membrane layer showed a free-defect structure, which corroborates with the result from the nitrogen adsorption. The scale of the outer surface image was at 20 μ m while the image was magnified at 500 X. It was suggested that the whitish surface as shown in Figure 10 is indicative of the mesoporous layer on the membrane surface.

Conclusion

The surface area and the pore size distribution of both modified and unmodified ceramic membranes were successfully determined using BET (specific surface area) and BJH (pore size distribution) methods. The surface area of the dip-coated silica membrane was higher (0.439m²/g) than the unmodified membrane support (0.206m²/g). The dip-coated silica membrane exhibited a type IV/V isotherm indicating that the membrane was mesoporous membrane at 77 K. However, the silica membrane exhibited a type III isotherm indicating a microporous membrane. The SEM of the silica membrane showed a defect-free layer as confirmed by the CO₂, N₂, Ar and He gas permeation results. The pore size distribution of the dip-coated membrane was also found to be greater (4.179nm) than the support (4.175nm) indicating the effect of the silica solution that was used in modifying the ceramic membrane. The gas permeance was found to decrease with increasing gauge pressure indicating Knudsen mechanism of gas transport. The gas flux increases linearly with increasing gauge pressure indicating viscous flow mechanism.

Acknowledgement

The Authors acknowledge the Center for Process Integration and Membrane Technology (CPIMT), School of Engineering, RGU, for providing the membrane and also the School of Pharmacy and Life Sciences RGU for the SEM images.

REFERENCES

- Choma J, Kloske M, Jaroniec M. 2003. An improved methodology for adsorption characterization of unmodified and modified silica gels. *Journal of Colloid and Interface Science*, 266(1), pp. 168-174.
- Coronas J, Santamaria J. 1999. Catalytic reactors based on porous ceramic membranes. *Catalysis Today*, 51(3), pp. 377-389.
- Dafinov A, Garcia-Valls R, Font J. 2002. Modification of ceramic membranes by alcohol adsorption. *Journal of Membrane Science*, 196(1), pp. 69-77.
- Kuraoka K, Chujo Y, Yazawa T. 2001. Hydrocarbon separation via porous glass membranes surface-modified using organosilane compounds. *Journal of Membrane Science*, 182(1), pp. 139-149.
- Lee D, Oyama ST. 2002. Gas permeation characteristics of a hydrogen selective supported silica membrane. *Journal of Membrane Science*, 210(2), pp. 291-306.
- Li K. Ceramic membranes for separation and reaction 2007. John Wiley and Sons Ltd, The Atrium, southern gate, Chichester, west sussex. PO198SQ, England.
- Marković A, Stoltenberg D, Enke D, Schlünder E, Seidel-Morgenstern A. 2009. Gas permeation through porous glass membranes: Part II: Transition regime between Knudsen and configurational diffusion. *Journal of Membrane Science*, 336(1), pp. 32-41.
- Peters T, Fontalvo J, Vorstman M, Keurentjes J. 2004. Design directions for composite catalytic hollow fibre membranes for condensation reactions. *Chemical Engineering Research and Design*, 82(2), pp. 220-228.
- Phattaranawik J, Jiratananon R, Fane A. 2003. Effect of pore size distribution and air flux on mass transport in direct contact membrane distillation. *Journal of Membrane Science*, 215(1) pp. 75-85.
- Sidhu PS, Cussler E. 2001. Diffusion and capillary flow in track-etched membranes. *Journal of Membrane Science*, 182(1) pp. 91-101.
- Smart S, Liu S, Serra JM, Diniz da Costa JC, Iulianelli A, Basile A. 2013. 8 - Porous ceramic membranes for membrane reactors. In: Basile A, editor. *Handbook of Membrane Reactors.: Wood head Publishing*, pp. 298-336.
- Tsai C, Tam S, Lu Y, Brinker CJ. 2000. Dual-layer asymmetric microporous silica membranes. *Journal of Membrane Science*, 169(2), pp. 255-268.
